

Differential Reactivities of Enyne Substrates in Ruthenium- and Palladium-Catalyzed Cycloisomerizations

Barry M. Trost,* Alicia C. Gutierrez, and Eric M. Ferreira

Department of Chemistry, Stanford University, Stanford, California 94305

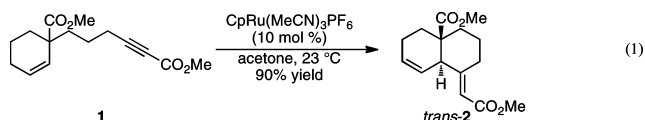
Received May 4, 2010; E-mail: bmtrost@stanford.edu

Abstract: Complementary methods for the transition-metal-catalyzed enyne cycloisomerizations of cyclic olefins have been developed. By using distinct ruthenium and palladium catalysts, decalins and 7,6-bicycles can be obtained with dichotomous stereochemical outcomes. The change in mechanism that accompanies the change in metal affords trans-fused 1,4-dienes with ruthenium and their cis-fused diastereomers under palladium catalysis. In the reactions under ruthenium catalysis, a coordinating group is required and acts to direct the metal to the same side of the carbocycle, resulting in the observed trans diastereoselectivity. Subtle changes in the carbocyclic substrate led to the discovery of a heretofore-unobserved mechanistic pathway, providing bicyclic cycloisomerization products under palladium catalysis and tricyclic products under ruthenium catalysis in *N,N*-dimethylacetamide (DMA). The differential effect of DMA supports a mechanism in which the coordination requirements of the two paths differ, allowing for the reaction to be shuttled through the metallacycle pathway (generating tricyclic products) when DMA is used as a solvent.

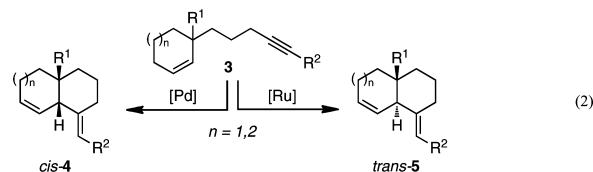
Introduction

A primary focus in our laboratory is the invention of transition-metal-catalyzed reactions for the rapid construction of molecular complexity from simple starting materials.¹ Of these, atom-economic reactions² — transformations that use only catalytic reagents and in which each atom of the starting materials is contained in the product — exemplify the ideal of efficient chemical synthesis. Developing methods that meet these criteria is desirable not only because such processes generate few byproducts but also because they make more efficient use of raw materials in an increasingly resource-conscious world.

A representative example of such a transformation is the cycloisomerization of enynes.³ Extending our previous work in this area to enynes containing cyclic olefins would allow access to fused carbocyclic ring systems (eq 1), chemical motifs that are abundant in naturally occurring, biologically active molecules. Recognizing, therefore, that the ability to rapidly construct fused five-, six-, and seven-membered ring systems would be an important synthetic tool and that control over the relative stereochemistry of fused ring junctions is a long-standing challenge in the synthetic community, we began a research program to study the reaction of cyclic olefin substrates (**1**) with a variety of transition-metal catalysts.



A preliminary account of these studies, detailing palladium- and ruthenium-catalyzed cycloisomerizations of six- and seven-membered carbocyclic enynes, was recently disclosed.⁴ Herein we present a full account of this work, which has resulted in the discoveries of (1) diastereoselective enyne cycloisomerizations to form bicycles that, depending on the metal catalyst, exclusively form either the cis- or trans-fused ring system (eq 2) and (2) reaction conditions that, depending on the metal catalyst, selectively yield either bi- or tricyclic products. These studies provide new insights into the mechanisms of these reaction manifolds, the implications of which are discussed.



Preparation of Enyne Substrates

The requisite enyne substrates can be readily prepared via a general synthetic plan that relies on the deconjugative alkylations of cyclic enoates.⁵ In the event, commercially available cyclohexene **6** was alkylated with iodides **7**, **8**, and **9** using LDA/

(1) For a review of atom-economic reactions developed in our laboratory, see: (a) Trost, B. M. *Acc. Chem. Res.* **2002**, *35*, 695–705. For reviews on non-metathesis, ruthenium-catalyzed carbon–carbon bond-forming reactions, see: (b) Trost, B. M.; Frederiksen, M. U.; Rudd, M. T. *Angew. Chem., Int. Ed.* **2005**, *44*, 6630–6666. (c) Trost, B. M.; Toste, F. D.; Pinkerton, A. B. *Chem. Rev.* **2001**, *101*, 2067–2096.

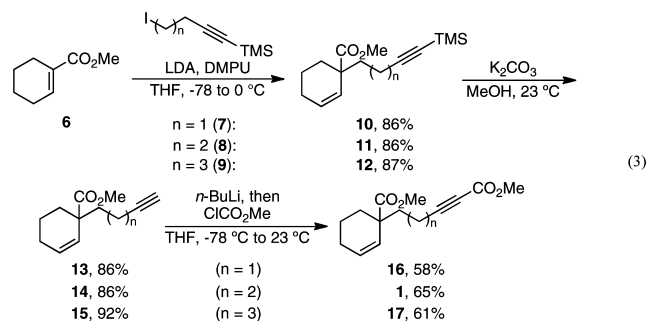
(2) Trost, B. M. *Science* **1991**, *254*, 1471–1477.

(3) For reviews on enyne cycloisomerizations, see: (a) Trost, B. M.; Krische, M. J. *Synlett* **1998**, 1–16. (b) Trost, B. M. *Acc. Chem. Res.* **1990**, *23*, 34–42. (c) Michelet, V.; Toullec, P. Y.; Genêt, J.-P. *Angew. Chem., Int. Ed.* **2008**, *47*, 4268–4315.

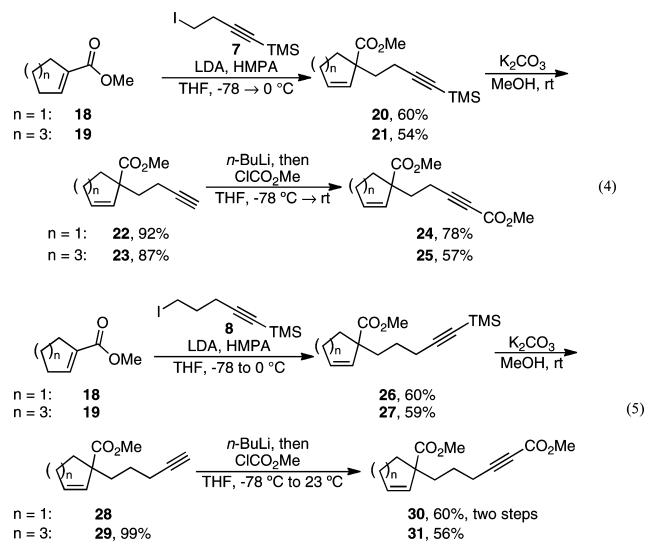
(4) Trost, B. M.; Ferreira, E. M.; Gutierrez, A. C. *J. Am. Chem. Soc.* **2008**, *130*, 16176–16177.

(5) (a) Herrmann, J. L.; Kieczkowski, G. R.; Schlessinger, R. H. *Tetrahedron Lett.* **1973**, *14*, 2433–2436. (b) Kuwajima, I.; Urabe, H. *Org. Synth.* **1988**, *66*, 87–94.

DMPU to provide esters **10**, **11**, and **12**, which vary only in their tether lengths (eq 3).



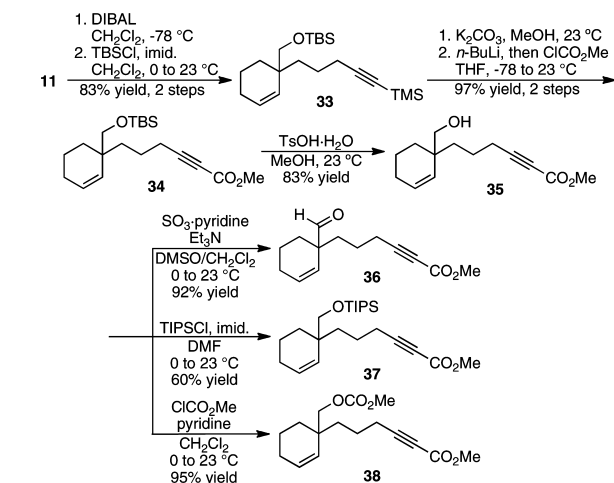
Substrates containing both larger and smaller ring sizes were also synthesized (eqs 4 and 5) following a similar protocol. Deconjugative alkylations of cyclopentene **18** and cycloheptene **19** were less effective than the alkylation of cyclohexene **6** but worked reasonably well using LDA/HMPA to afford enynes **20** and **21** from iodide **7**, and enynes **26** and **27** from iodide **8**.⁶



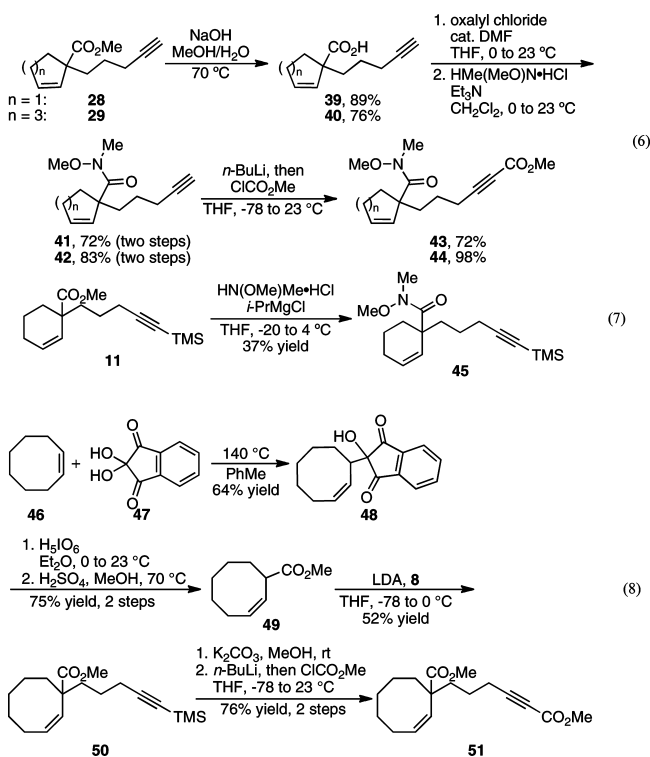
The silylated esters obtained from the deconjugative alkylation (**10**–**12** and **26**–**27**) and their desilylated analogues (**13**–**15**, **22**, **23**, **28**, and **29**) were used to access an array of substrates via conventional methods. The synthetic routes to enynes **34**–**38** from precursor **11** are illustrated in Scheme 1; the cyclopentene- and cycloheptene-derived congeners were made analogously.⁷

Enynes containing an amide at the quaternary position were synthesized via standard conditions (eq 7). Cyclooctene substrate **50** could not be synthesized using deconjugative alkylation, likely owing to the conformational restrictions caused by transannular interactions in a cyclooctyl ring. Instead, β,γ -unsaturated ester **49** was synthesized using a ninhydrin ene reaction reported by Gill et al.,⁸ followed by

Scheme 1. Substrate Syntheses



oxidative cleavage⁹ and subsequent Fischer esterification (eq 8). Alkylation and functional group manipulation provided enyne **51**.



Cycloisomerizations

6,6- and 7,6-Bicyclic Structures. We began by studying the cycloisomerization of enyne **1** using our standard conditions for ruthenium-catalyzed alkene–alkyne couplings (5 mol % CpRu(MeCN)₃PF₆ in acetone at ambient temperature). The reaction afforded bicycle **2** in 90% yield (Table 1, entry 1). Remarkably, the transformation was completely diastereoselective for the trans-fused ring system.

This result is particularly noteworthy because more classical ways of making decalins, such as cycloalkylations, generally lead to cis-fused bicycles.¹⁰ The more commonly employed

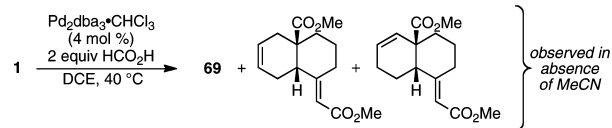
(6) The deprotonation was complicated by competitive conjugate addition of diisopropylamide into **8**, even when using HMPA.

(7) See Supporting Information.

(8) Gill, G. B.; Idris, M. S. H.; Kirolos, K. S. *J. Chem. Soc., Perkin Trans. 1* **1992**, 2355–2365.

(9) Gill, G. B.; Idris, M. S. H.; Kirolos, K. S. *J. Chem. Soc., Perkin Trans. 1* **1992**, 2367–2369.

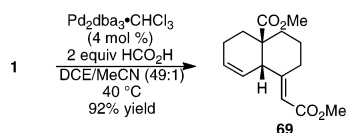
Scheme 2. Undesired Olefin Isomerization



cycloisomerization,¹² ester **1** was examined. Highest conversions were obtained when HCO₂H was used in combination with DCE as the solvent. Variations to this system (e.g., AcOH in place of HCO₂H or benzene instead of DCE as the solvent) led to diminished reactivity.

In our initial studies, concomitant formation of olefin isomers prevented us from obtaining the desired 1,4-diene in acceptable yields (Scheme 2). Gratifyingly, the addition of 2 vol % acetonitrile prevented the formation of these byproducts (Scheme 3).¹³ These optimized conditions (4 mol % Pd₂dba₃·CHCl₃, 2 equiv HCO₂H, DCE, 2 vol % acetonitrile, 40 °C, Scheme 3) were applied to all of our subsequent palladium-catalyzed cycloisomerizations.

Scheme 3. Optimized Pd-Catalyzed Cycloisomerization

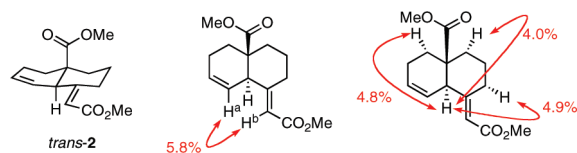


The cyclic enynes used to illustrate the scope of the ruthenium-catalyzed reaction (Table 1) were also cycloisomerized under palladium catalysis. The corresponding 6,6- and 7,6-cis-fused bicycles were obtained in high yields, and, in contrast to the ruthenium-catalyzed process, in this palladium-catalyzed reaction they were obtained with complete diastereoselectivity for the *cis* isomers (Table 2).

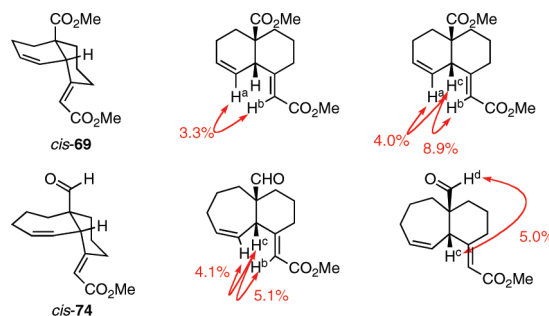
A variety of functional groups are tolerated by the palladium catalyst, with the exception of acid **57** (entry 3) and ynamide **52** (entry 6). Aldehydes (entries 2 and 9), amides (entries 5 and 10), and ynones (entry 7) underwent the cycloisomerization in excellent yields and diastereoselectivity. In contrast to the slow reactivity observed under ruthenium catalysis, under palladium catalysis alcohol **35** underwent facile cyclization to generate bicycle *cis*-**73** in less than 3 h (entry 4).

The relative stereochemistry of the products was determined by examination of key coupling constants and nuclear Overhauser effect (NOE) enhancements (Figures 2 and 3). In all cases, the double-bond geometry was secured by observing NOEs between H^a and H^b. COSY spectra were used to correlate chemical shift with connectivity. The differences between the NOEs observed for *trans*-**2** and those observed for *cis*-**69** constitute strong evidence for our stereochemical assignment.

For the *trans*-fused series, a strong NOE enhancement was measured between the doubly allylic proton (H^c) and the other axial protons (illustrated for *trans*-**69** in Figure 2). In contrast, strong NOE enhancements were observed between H^c and the

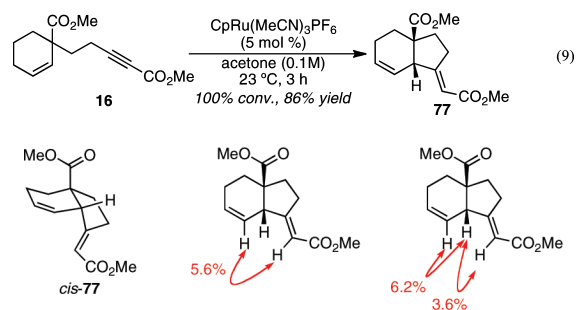
Figure 2. Stereochemical assignment of *trans*-**2**.

vinyl protons (H^a and H^b) for the *cis*-fused bicycles. Representative examples are illustrated for *cis*-**69** and *cis*-**74** (Figure 3). In addition to H^b–H^c enhancements, the strong NOE enhancement between the aldehydic proton H^d and H^c of *cis*-**74** is highly diagnostic and further confirms our assignments.

Figure 3. Representative stereochemical assignments of *cis* bicycles.

6,5-Bicyclic System. Decreasing the tether length by one carbon allowed us to examine the formation of five-membered rings from cyclohexene- and cycloheptene-containing enynes, which would produce 6,5- and 7,5-bicycles, respectively.

The formation of 6,5-bicycles via ruthenium-catalyzed cycloisomerization was probed using enyne **16**. In the event, 6,5-bicycle **77** was isolated in 86% yield as a single diastereomer (eq 9). Notably, ¹H NMR studies revealed that the product contained a *cis* ring fusion (Figure 4). Unfortunately, attempts to form analogous 7,5-bicycles were not successful.¹⁴

Figure 4. Stereochemical NOE analysis of **51**.

6,7-System. Attempts to form seven-membered rings via ruthenium-catalyzed cycloisomerization revealed a limit of this catalytic system. While small amounts of 6,7-bicycle **79** could be observed, cycloisomerization did not occur catalytically, even under forcing conditions (Table 3). After increasing both the temperature to 60 °C and the catalyst loading to 30 mol %, at the end of 24 h the reaction had only reached 33% conversion (entry 4), representing a reaction with minimal catalyst turnover.

(12) (a) Trost, B. M.; Tanoury, G. J.; Lautens, M.; Chan, C.; MacPherson, D. T. *J. Am. Chem. Soc.* **1994**, *116*, 4255–4267. (b) Trost, B. M.; Romero, D. L.; Rise, F. *J. Am. Chem. Soc.* **1994**, *116*, 4268–4278. (c) Trost, B. M.; Li, Y. *J. Am. Chem. Soc.* **1996**, *118*, 6625–6633.

(13) Analogous olefin isomerization is often observed in intramolecular palladium-catalyzed Heck reactions of cyclic olefins. Silver or thallium salts, commonly employed as additives to suppress these isomerizations, were ineffective. See: Link, J. T. *Org. React.* **2002**, *60*, 157–534.

(14) Cycloheptene **25** was found to be unreactive to our optimized conditions. While 25% conversion to an unidentified product was observed upon heating to 45 °C, none of the desired 7,5-bicycle was formed.

Table 2. 6,6- and 7,6-Bicycles via Pd-Catalyzed Cycloisomerizations

entry	substrate	product	yield, time (%), h ^a	dr ^b	entry	substrate	product	yield, time (%), h ^a	dr ^b
1			92, 4	> 19 : 1	6		—	NR	—
2			73, 5	> 19 : 1	7			67, 12	> 19 : 1
3		—	NR	—	8			95, 3	> 19 : 1
4			83, 2.5	> 19 : 1	9			92, 4	> 19 : 1
5			68, 15	> 19 : 1	10			95, 2.5	> 19 : 1

^a Isolated yield. NR: no reaction. ^b Determined by ¹H NMR.

Table 3. Behavior of the 6,7-System

entry	conditions	catalyst loading (mol %)	results ^a
1	2.5 h, 23 °C	5	no reaction
2	3 h, 45 °C	5	17% conv
3	6 h, 45 °C	20	25% conv
4	24 h, 60 °C	30	33% conv

^a Determined by ¹H NMR of crude reaction.

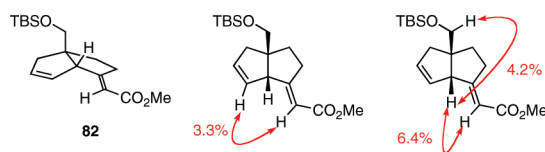
5,*n*-Bicycles. The excellent yields and diastereoselectivities with which the 6,6- and 7,6-ring systems were obtained led us to investigate the formation of 5,*n*-ring systems. Toward this end, enynes **24** and **80** were subjected to the ruthenium-catalyzed cycloisomerization reaction conditions. Ester **24** underwent smooth cyclization to the 5,5-bicyclic product (**81**), with complete selectivity for the *cis* diastereomer (Table 4, entry 1). Enyne **80**, containing a silyl ether at the quaternary carbon, also underwent cyclization to generate the *cis*-fused product **82** under ruthenium catalysis (entry 2). The relative stereochemistry of the bicyclic products was secured by an analysis of the COSY spectrum along with the NOE enhancements illustrated in Figure 5.

Extending the alkyne tether by one carbon in order to form the 5,6-bicycle had a profound impact on the reaction. When substrate **30** was submitted to the optimized palladium-catalyzed reaction conditions, the expected bicycle **83** was formed in excellent yield as a single diastereomer (Scheme 4). To our

Table 4. Ru-Catalyzed Cycloisomerizations To Form 5,5-Bicycles

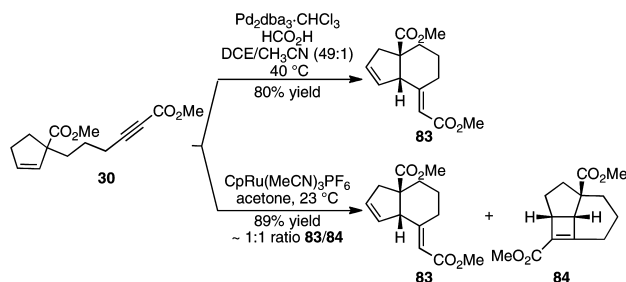
entry	substrate	product	conversion (%) ^a	yield (%) ^b	dr ^a
1			100	81	> 19:1
2			100	85	> 19:1

^a Determined by ¹H NMR. ^b Isolated yield.

**Figure 5.** Representative stereochemical assignment.

surprise, when **30** was submitted to the ruthenium-catalyzed reaction conditions, bicycle **83** was formed in equal amounts along with tricycle **84**. Both products were formed as single diastereomers.

A similar [2+2] cycloaddition with iodoenynes was recently reported by Fürstner, in which the pentamethylcyclopentene (Cp*) analogue of our catalyst, Cp*₂Ru(MeCN)₃PF₆, was em-

Scheme 4. Novel Tricyclic Product Obtained under Ruthenium Catalysis

ployed.¹⁵ When enyne **30** was submitted to the conditions reported by Fürstner (catalytic $\text{Cp}^*\text{Ru}(\text{MeCN})_3\text{PF}_6$ in dimethylformamide (DMF) at room temperature), no reaction was observed.

The nickel-catalyzed [2+2] cycloaddition of 1,2-diphenylethyne and 2,5-norbornadiene (NBD) reported by Schrauzer in 1964¹⁶ was the first transition-metal-catalyzed alkyne–olefin [2+2] addition. Since Schrauzer's initial report, palladium,¹⁷ platinum,¹⁸ cobalt,¹⁹ gold,²⁰ rhodium,²¹ rhenium,²² ruthenium,²³ iridium,²⁴ and molybdenum²⁵ have all been shown to catalyze the cycloaddition of an alkyne and an olefin. However, despite the array of metal complexes that have been employed for this transformation, this reactivity is unprecedented for the $\text{CpRu}(\text{MeCN})_3\text{PF}_6$ catalyst.

Under the standard conditions (5 mol % $\text{CpRu}(\text{MeCN})_3\text{PF}_6$, acetone, 23 °C, 2 h), a 1:1 mixture of bicycle and tricycle was obtained in high yields for all of the substrates examined (Table 5).

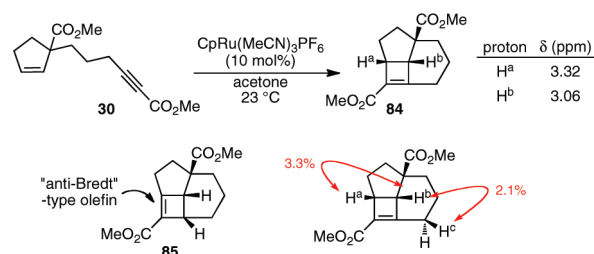
It is believed that cyclobutene **84** as drawn is the product characterized. Correlations between chemical shift and connectivity were deduced by COSY analysis. Proton NMR studies show an NOE enhancement between H^a and H^b , as would be expected for two cis protons (Scheme 5). An NOE enhancement

Table 5. Cycloisomerizations under Standard Conditions

entry	R ¹	R ²	conversion (%)	ratio tricycle/bicycle ^a	yield (tricycle, bicycle, %) ^b
1	CO ₂ Me	CO ₂ Me	100	~1:1	89 ^c
2	CH ₂ OH	CO ₂ Me	100	~1:1	43, 53
3	CH ₂ OTBS	CO ₂ Me	100	~1:1	46, 42
4	CH ₂ OAc	CO ₂ Me	100	~1:1	30, 38
5	CHO	CO ₂ Me	100	~1:1	49, 50
6	CH ₂ OTBDPS	CHO	100	~1:1	98 ^c
7	CH ₂ OBn	CHO	100	~1:1	90 ^c

^a Determined by ¹H NMR of crude reaction. ^b Isolated yield. ^c Isolated as a mixture of tricycle and bicycle.

is also observed between the methylene proton H^c and H^b . Importantly, the chemical shifts of these diagnostic cyclobutene protons correlate with the values reported for similar tricyclic cyclobutenes formed under platinum catalysis.²⁶ Moreover, if the ester were unsaturated in the other direction of the cyclobutene, that compound (**85**) would contain a highly strained olefin.²⁷

Scheme 5

Given that we could access the bicycle exclusively via palladium catalysis, we then sought reaction conditions to provide the tricycle exclusively under ruthenium catalysis (Scheme 6). We began our optimization studies with enyne **30**.

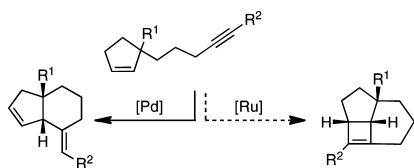
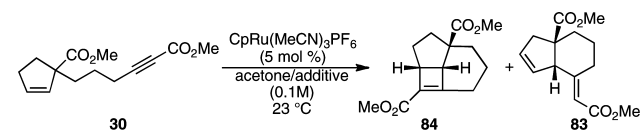
Reasoning that the introduction of another coordinating solvent with different ligating properties might affect the selectivity of the reaction, we examined a variety of solvents. Unfortunately, none of the additives (acetic acid, dioxane, ethyl acetate, methanol) increased the selectivity for either product (Table 6). Toluene (Table 6, entry 4) and dimethylsulfoxide (DMSO) (Table 6, entry 6) completely shut down the reaction, while the introduction of acetonitrile decreased the reaction conversion to 44%. The addition of nitromethane proved to be differential, providing tricycle **84** in a slight excess relative to bicycle **83** (Table 6, entry 10).

This promising result led us to examine DMF, a solvent that we have previously shown is compatible for reactions with $\text{CpRu}(\text{MeCN})_3\text{PF}_6$. In this case, when DMF was

- (15) Fürstner, A.; Schlecker, A.; Lehmann, C. W. *Chem. Commun.* **2007**, 4277–4279.
- (16) Schrauzer, G. N.; Glockner, P. *Chem. Ber.* **1964**, 97, 2451–2462.
- (17) (a) Coulson, D. R. *J. Org. Chem.* **1972**, 37, 1253–1254. (b) Trost, B. M.; Trost, M. K. *Tetrahedron Lett.* **1991**, 32, 3647–3550. (c) Trost, B. M.; Yanai, M.; Hoogsteen, K. *J. Am. Chem. Soc.* **1993**, 115, 5294–5295.
- (18) (a) Bajracharya, G. B.; Nakamura, I.; Yamamoto, Y. *J. Org. Chem.* **2005**, 70, 892–897. (b) Fürstner, A.; Davies, P. W.; Gress, T. *J. Am. Chem. Soc.* **2005**, 127, 8244–8245. (c) Matsuda, T.; Kadowaki, S.; Goya, T.; Murakami, M. *Synlett* **2006**, 575–578.
- (19) (a) Chao, K. C.; Rayabarapu, D. K.; Wang, C.-C.; Cheng, C.-H. *J. Org. Chem.* **2001**, 66, 8804–8810. (b) Treutwein, J.; Hilt, G. *Angew. Chem., Int. Ed.* **2008**, 47, 6811–6813.
- (20) (a) Nieto-Oberhuber, C.; Lopez, S.; Echavarren, A. M. *J. Am. Chem. Soc.* **2005**, 127, 6178–6179. (b) Odabachian, Y.; Gagosz, F. *Synth. Catal.* **2009**, 351, 379–386. (c) Oh, C. H.; Kim, A. *Synlett* **2008**, 777–781.
- (21) Shibata, T.; Takami, K.; Kawachi, A. *Org. Lett.* **2006**, 8, 1343–1345.
- (22) Kuninobu, Y.; Yu, P.; Takai, K. *Chem. Lett.* **2007**, 36, 1162–1163.
- (23) (a) Mitsudo, T.; Kokuryo, K.; Takegami, Y. *J. Chem. Soc., Chem. Commun.* **1976**, 722–723. (b) Mitsudo, T.; Kokuryo, K.; Shinsugi, T.; Nakagawa, Y.; Watanabe, Y.; Takegami, Y. *J. Org. Chem.* **1979**, 44, 4492–4496. (c) Mitsudo, T.; Hori, Y.; Watanabe, Y. *J. Organomet. Chem.* **1987**, 334, 157–167. (d) Mitsudo, T.; Naruse, H.; Kondo, T.; Ozaki, Y.; Watanabe, Y. *Angew. Chem., Int. Ed. Engl.* **1994**, 33, 580–581. (e) Jordan, R. W.; Tam, W. *Org. Lett.* **2000**, 2, 3031–3034. (f) Jordan, R. W.; Tam, W. *Org. Lett.* **2001**, 3, 2367–2370. (g) Tenaglia, A.; Giordano, L. *Synlett* **2003**, 2333–2336. (h) Villeneuve, K.; Tam, W. *Organometallics* **2006**, 25, 843–848. (i) Reference 15. (j) Saito, N.; Tanaka, Y.; Sato, Y. *Organometallics* **2009**, 28, 669–671.
- (24) Fan, B.-M.; Li, X.-J.; Peng, F.-Z.; Zhang, H.-B.; Chan, A. S. C.; Shao, Z.-H. *Org. Lett.* **2009**, 12, 304–306.
- (25) Shen, Q.; Hammond, G. B. *J. Am. Chem. Soc.* **2002**, 124, 6534–6535.

(26) See ref 18b.

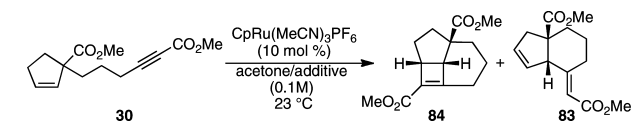
(27) The smallest carbocycle that can contain a trans-olefin has been the subject of continuing interest in organic chemistry. While trans-cyclooctene is fairly stable (strain energy ~16 kcal/mol), trans-cycloheptene is significantly higher in energy (~27 kcal/mol) and has only been isolated at low temperatures. For a complete discussion, see: Anslyn, E. V.; Dougherty, D. A. *Modern Physical Organic Chemistry*; University Science Books: New York, NY, 2006.

Scheme 6. Desired Catalyst-Controlled Product Selectivity**Table 6.** Solvent Screen

entry	solvent additive	conversion (%) ^a	ratio tricycle/bicycle ^a
1	2.5 vol % AcOH	100	1:1
2	20 vol % AcOH	100	1:1
3	20 vol % dioxane	100	1:1
4	20 vol % toluene	NR	
5	20 vol % EtOAc	100	1:1
6	20 vol % DMSO	NR	
7	20 vol % MeCN	44	1:1
8	2.5 vol % MeOH	100	1:1
9	50 vol % CH ₂ Cl ₂	100	1:1
10	20 vol % MeNO ₂	100	1.2:1

^a Determined by ¹H NMR of crude reaction. NR: no reaction.

employed as a solvent, the reaction did not proceed at all after 3 h at 23 °C. The addition of 2 vol % DMF to an acetone solution of substrate and catalyst (Table 7, entry 1) slowed the reaction, but cyclobutene formation occurred in more than 2-fold excess relative to bicycle formation. Further increasing the amount of DMF relative to acetone led to a moderate increase in selectivity (Table 7, entry 2), but use of greater than 20 vol % DMF decreased the conversion significantly (Table 7, entry 3).

Table 7. Nitrogen-Based Solvent Screen

entry	solvent additive	time (h)	conversion (%) ^d	ratio tricycle/bicycle ^d
1	2 vol % DMF	15	100	2.4:1
2	20 vol % DMF	13	80	3:1
3	50 vol % DMF	13	67	3:1
4	5 vol % NMP	4	100	3.6:1
5 ^a	10 vol % NMP	3	100	5:1
6 ^a	20 vol % NMP	3	100	3:1
7	50 vol % DMA	15	48	10:1
8	80 vol % DMA	18	63	14.6:1
9	100 vol % DMA	18	74	15.2:1
10 ^{b,c}	100 vol % DMA	12	93	12.5:1
11 ^b	20 vol % NMP, 80 vol % DMA	16	78	7:1
12 ^b	10 vol % NMP, 80 vol % DMA	12	40	10.3:1

^a Using 20 mol % catalyst. ^b Using 15 mol % catalyst. ^c Reaction conducted at 40 °C. ^d Determined by ¹H NMR of crude reaction

Hoping that an alternative nitrogen-based solvent might similarly favor formation of cyclobutene **84**, we tested *N*-methylpyrrolidone (NMP), nitromethane, and *N,N*-dimethylacetamide (DMA) as additives (Table 7, entries 4–12). The use of NMP resulted in faster reaction rates but with modest product selectivity (entries 5 and 6). The highest

product selectivity was obtained with 100 vol % DMA at room temperature (entry 9); however, the reaction stopped at 74% conversion. Raising the temperature to 40 °C increased the conversion to 93% while only slightly decreasing the selectivity (entry 10). These conditions (15 mol % CpRu(MeCN)₃PF₆, DMA, 40 °C), the best compromise between conversion and selectivity, were then adopted as the optimized conditions for tricycle formation.

Using these optimized conditions, a variety of substrates were examined (Table 8). Free alcohols (Table 8, entry 2) and aldehydes (Table 8, entry 3) are tolerated, generating the corresponding cyclobutenes in excellent yields. In contrast to the cycloisomerization reaction to form 6,6- and 7,6- bicycles, this system tolerates a wider variety of functional groups, such as silyl ethers (Table 8, entries 4, 6, and 7) and ynals (Table 8, entries 4, 5, and 8).

Complementary product selectivity can be obtained simply by changing the catalyst from ruthenium to palladium. To demonstrate this, the substrates were also subjected to the palladium-catalyzed cycloisomerization conditions. We were pleased to find that the reaction produced the desired cis-fused bicycles in good to excellent yields with complete diastereoselectivity (Table 9).

Carbonate **111**, silyl ether **112**, and alcohol **113** (Figure 6) were unreactive to ruthenium catalysis as well. In separate experiments, increasing the temperature of the standard reactions (in acetone) to 50 °C did not improve the conversion.

Not all of the substrates examined cyclized successfully under ruthenium catalysis. Curiously, Weinreb amide **43**, the cyclopentene analogue of **63** and **44**, was not reactive. Under the standard reaction conditions (acetone, 23 °C), the reaction with amide **43** failed to go to complete conversion after 3.5 h (standard reaction time 2 h). Additionally, under these standard conditions, amide **43** was the only substrate to give an unequal mixture of bi- and tricyclic products, producing the two in a 1:4 ratio, respectively (Table 10, entry 1). In DMA, conversion was only 42% after 11 h at 40 °C (entry 2), and after 24 h only 50% (entry 3). Repeated attempts to separate the tricycle from the starting material were not successful, and the isolation of tricycle **109** was ultimately abandoned.

As had been observed previously, enynes containing an alkyne terminated by a group other than an electron-withdrawing group were completely unreactive (Figure 7). Ynamide **52** and ynone **55** (Table 1, entries 6 and 7), used as substrates for generating the 6,6-bicyclic products, required more forcing conditions. We reasoned that if the (unknown) factors that slowed the cycloisomerization of these enynes were present in the 5,6-system, a change in product ratio might result, favoring the cyclobutene product. Instead, reactions with 5,6-ynone **114** and ynamide **115** were even more sluggish than those with their 6,6-analogues (Scheme 7).

To determine if these optimized conditions (15 mol % CpRu(MeCN)₃PF₆, DMA, 40 °C) were unique to 5,6-congeners, substrates from the 6,6- and 6,7-systems (esters **52** and **31**) were submitted to the reaction under the same conditions. No reaction was observed after 12 h (eq 10), indicating that the formation of tricyclic products is indeed unique to the 5,6-system.

Mechanistic Considerations: Palladium Catalysis. The cis-selectivity observed in the palladium-catalyzed cycloisomerization can be explained by a mechanism in which the metal is directed to the same side of the ring as the alkyne (Scheme 8). The active catalyst is generated by oxidative insertion of

Table 8. Cycloisomerizations under Tricycle-Optimized Conditions

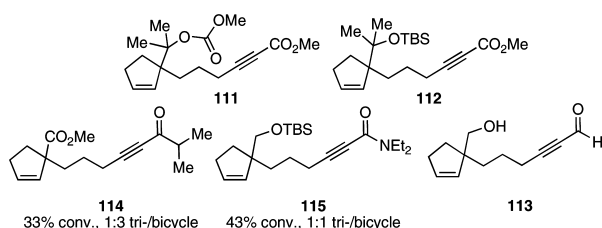
entry	substrate	product	yield(%) ^a	tricycle/ bicycle ^b	entry	substrate	product	yield(%) ^a	tricycle/ bicycle ^b
1			91	12.5:1	5			81 ^c	8.3:1
2			71	2.7:1	6			91	10.4:1
3			89	14.2:1	7			91	10.7:1
4			61	>19:1	8			66	10.8:1

^a Yield of isolated tricycle. ^b Determined by ¹H NMR. ^c Isolated as an inseparable, 8.3:1 mixture of tricycle and bicycle.

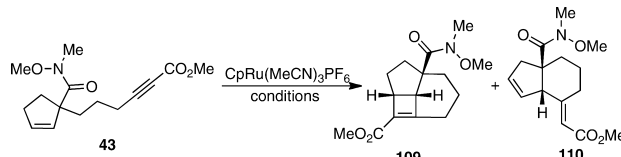
Table 9. 5,6-Cis-Fused Bicycles via Pd-Catalyzed Cycloisomerizations

entry	substrate	product	yield(%) ^a	dr ^b	entry	substrate	product	yield(%) ^a	dr ^b
1			80	> 19:1	5			47 ^c	> 19:1
2			97	> 19:1	6			91	> 19:1
3			81	> 19:1	7			99	> 19:1
4			57	>19:1	8			80	> 19:1

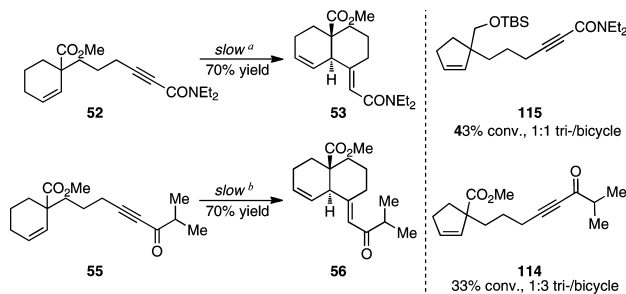
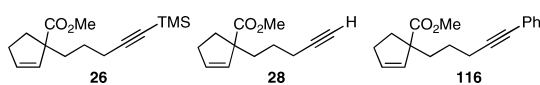
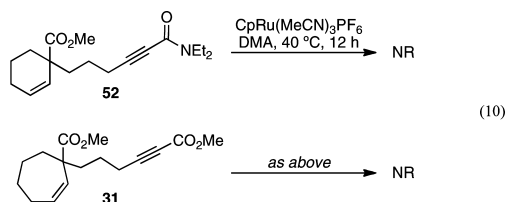
^a Isolated yield. ^b Determined by ¹H NMR. ^c Isolated along with 23% of olefin-isomerized 1,5-diene.

**Figure 6.** Unproductive enynes with electron-deficient alkynes.

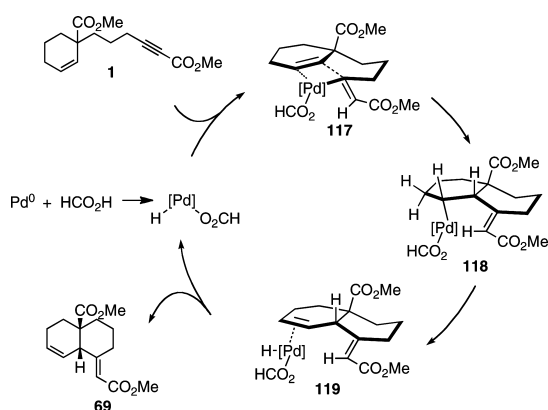
palladium(0) into HCO₂H to generate a palladium(II) species that then hydrometalates the alkyne to form vinylpalladium species **117**. Intramolecular binding and insertion of the olefin then provides intermediate **118**. Subsequent β -hydride elimination produces the 1,4-diene product, which is still bound to the palladium through η^2 -coordination of the newly formed olefin **119**. The concomitant formation of olefin isomers observed in our initial studies is hypothesized as arising from palladium hydride insertion–elimination pathways at this

Table 10. Behavior of Weinreb Amide


entry	conditions	time (h)	conversion (%) ^a	ratio 109/110
1	acetone, 23 °C	3.5	71	4:1
2	DMA, 40 °C	11	42	8:1
3	DMA, 40 °C	24	50	nd ^b

^a Determined by ¹H NMR. ^b Not determined.**Scheme 7.** Relatively Slower Reactivity of **115** and **114**^a Using 10 mol % CpRu(MeCN)₃PF₆ in acetone at 40 °C. ^b Reaction time was 6 h using 20 mol % CpRu(MeCN)₃PF₆ in acetone at 23 °C.**Figure 7.** Unreactive substrates with electron-rich alkynes.

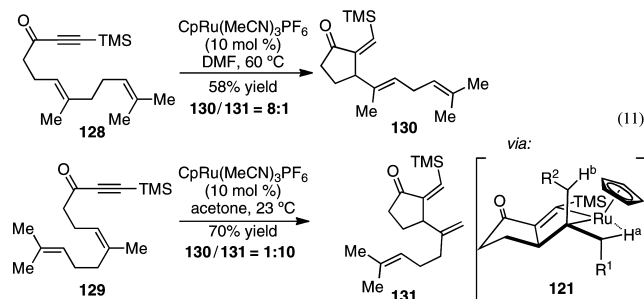
step. The introduction of acetonitrile facilitates decomplexation of the product via ligand exchange (**119** → **69**).

Scheme 8. Proposed Pd-Cycloisomerization Catalytic Cycle

Mechanistic Considerations: Ruthenium Catalysis. Electronic Requirements. The sum of our studies on this catalyst system — both these current studies and the studies of noncyclic

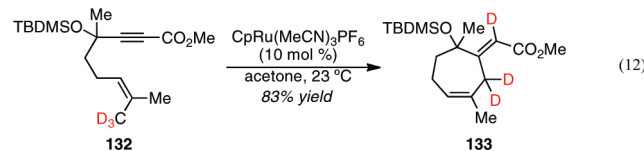
enyne²⁸ previously reported — suggest that there are two operative mechanisms in enyne cycloisomerizations catalyzed by CpRu(MeCN)₃PF₆: C–H insertion and metallacycle formation. The operable, productive mechanism for a given enyne is dictated by its olefin geometry. The data suggest that, for enynes containing (*E*)-olefins, cycloisomerization proceeds via a ruthenacycle, while enynes containing (*Z*)-olefins undergo an allylic C–H insertion. The two reaction manifolds are illustrated in Scheme 9. In path A, initial binding is followed by reversible metallacycle formation (**120a** → **121a**). β-Hydride elimination from the pseudoequatorial substituent generates a vinyl ruthenium hydride (**122**) that undergoes reductive elimination, yielding the cyclized product **123** and regenerating the catalyst.

Evidence that β-hydride elimination occurs toward the trans substituent (**CH₂R¹** in metallacycle **121a**, corresponding to the pseudoequatorial position) was provided by the cycloisomerizations of geranyl-derived enyne **128** and neryl-derived enyne **129** (eq 11). β-Hydride elimination occurred regioselectively from the (*E*)-substituent to provide the corresponding cyclopentanones **130** and **131**. The product ratios indicate that, while elimination toward the cis substituent is possible, it is the higher-energy pathway.



In the case of (*Z*)-olefins (**120b**, Scheme 9), the unfavorable orbital overlap in metallacycle **121b** between the metal and H^b, the hydrogen required for β-elimination from the intermediate ruthenacyclopentene, prevents the reaction from proceeding forward along this pathway. (*Z*)-Olefins thus react according to an alternative mechanism (path B). In this case, initial allylic C–H activation provides ruthenium–allyl species **124** that undergoes an intramolecular 1,4-addition to the alkyne, forming vinylruthenium **125**. Reductive elimination affords diene **127** and regenerates the active catalyst **126**.

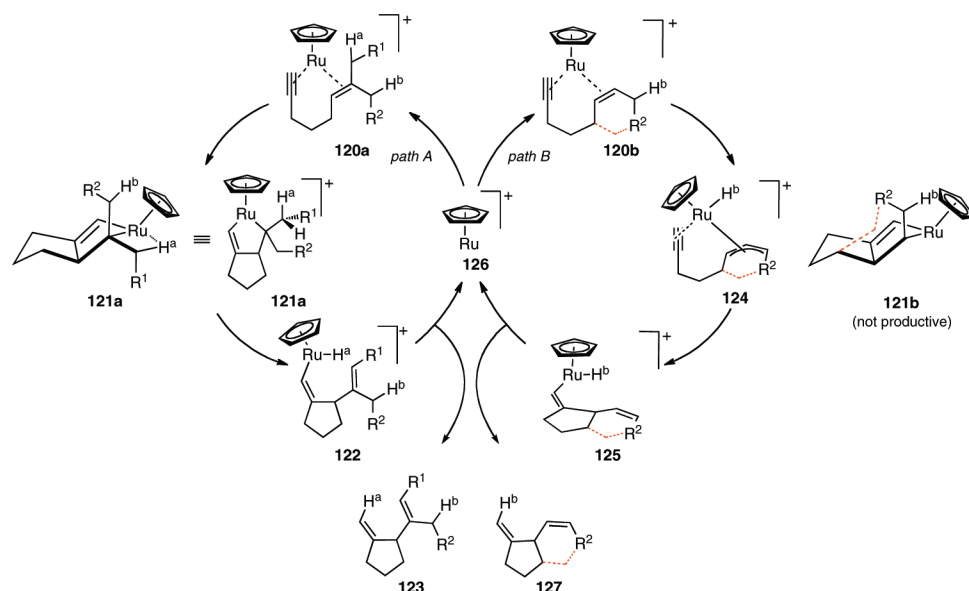
Evidence for this dichotomy was provided by deuterium-labeling studies, wherein a substrate (**132**) sterically prohibited from undergoing metallacycle formation underwent allylic C–H insertion exclusively into the cis-methyl substituent (eq 12).



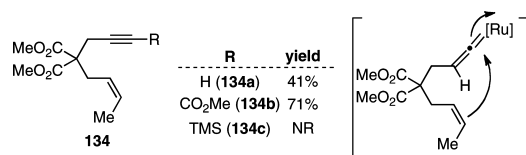
Lastly, careful examination of the dependence of reactivity on the alkyne substitution pattern of the following enynes reveals an interesting pattern. The series of enynes containing (*Z*)-olefins that were examined in our previous study and the

(28) (a) Trost, B. M.; Toste, F. D. *J. Am. Chem. Soc.* **1999**, *121*, 9728–9729. (b) Trost, B. M.; Toste, F. D. *J. Am. Chem. Soc.* **2002**, *124*, 5025–5036.

Scheme 9. Possible Mechanistic Manifolds

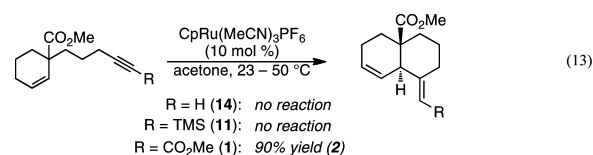


yields of the corresponding diene products are depicted in Figure 8. The series of enynes, also containing (*Z*)-olefins, examined as part of this current study are illustrated in eq 13. The difference in reactivity between terminal alkyne **134a** and TMS alkyne **134c** is intriguing. Specifically, the failure of cyclohexenyl **14**, which, like enyne **134a**, is also a 1,6-enyne containing a terminal alkyne and a *cis*-olefin, is difficult to explain. If the metallacycle derived from terminal alkyne **134a** is somehow able to achieve the requisite metal– β -hydride orbital overlap at higher temperatures, it is odd that neither silyl-enyne **134c** nor cyclic **14** does.

Figure 8. Reactivity of (*Z*)-olefin-containing enynes.

One possible explanation for these observations is that the terminal alkyne in **134a** is somehow facilitating an *in situ* olefin isomerization, to the corresponding *trans*-olefin, which then cycloisomerizes via the metallacycle pathway. If the terminal alkyne, via vinylidene formation, for instance, aids in this geometrical isomerization process, it would explain the inability the silyl alkyne to undergo cyclization. Additionally, it would explain why the cyclic olefin-containing enynes, whose olefins are geometrically constrained, do not react.

As noted previously, silyl alkyne **11** and terminal alkyne **14** were completely unreactive (eq 13), while analogous substrate **1**, featuring a methyl ester at the alkyne terminus, afforded the desired 1,4-diene in excellent yield as a single diastereomer (eq 13 and Table 1, entry 1). The reactivities of both of these cyclic substrates and of linear enynes **134a–c** can be rationalized by a C–H insertion mechanism (path B, Scheme 9), wherein the nature of the carboruthenation step (**124** \rightarrow **125**) is akin to the conjugate addition of a metal–alkyl species to an unsaturated carbonyl. The reaction cannot occur, therefore, if the alkyne is not a 1,4-acceptor (i.e., terminated by an electron-withdrawing group).²⁹

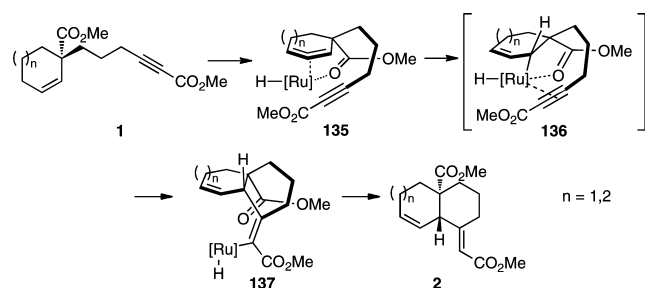


The failure of enynes **111** and **112** (Figure 6) to react is likely due to the steric demand of the functional groups (a tertiary carbonate in **111** and a tertiary ether in **112**) at the quaternary center in both enynes. Van der Waals interactions between the tertiary ether and one of the methylene groups in the side chain might prevent the pendant alkyne from achieving the orientation required for orbital overlap that would lead to further reaction.

Trans Diastereoselectivity: 6,6- and 7,6-Bicycles. Although the aforementioned facets of this chemistry explain reactivity, they do not explain diastereoselectivity. We had anticipated generation of the *cis*-fused decalin system, expecting that a coordinated alkyne would direct allylic C–H activation. However, carbon–carbon bond formation occurs *syn* to the ester, which implies that the C–H insertion must also occur on the same face. It appears, therefore, that the carbonyl moiety is acting to direct the formation of the intermediate allylruthenium species (Scheme 10). Carbonyl-directed η^3 -allyl formation (**135**) is followed by ligand exchange to form alkynyl-coordinated **136**, in which the metal is bound to the carbocycle in an η^1 manner; subsequent carboruthenation and reductive elimination produce the observed diastereomer (*trans*-**2**).

Further insights into our understanding of this reaction were provided by other substrates. Silyl ether **37** (see Figure 1), bearing a non-coordinating moiety at the quaternary carbon, was completely unreactive to these enyne cycloisomerizations, even with higher catalyst loadings and at elevated temperatures. Nitrile **66** was also unreactive, suggesting that C–H insertion to form the metal allyl species was due not solely to an inductive effect of the key functional group, but also to a specific Lewis

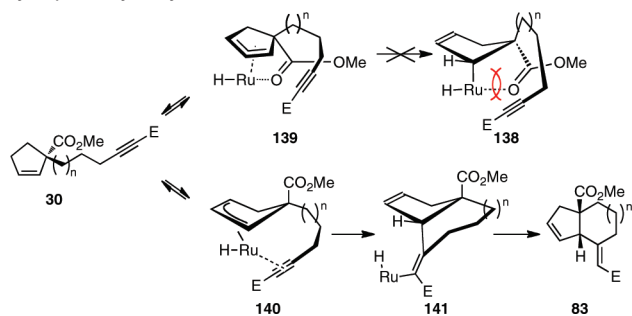
(29) These requirements do not apply to the palladium-catalyzed reaction. For example, under palladium catalysis the cycloisomerization of enyne **14** is a facile process (100% conversion, 64% yield, isolated as an inseparable 8:2 mixture of expected bicycle and olefin-isomerized 1,5-diene, unoptimized). See ref 3b for additional examples.

Scheme 10. Source of Trans Diastereoselectivity

basicity. The lack of reactivity observed for carbonate **38** is also understood in terms of this proposed mechanism. While the carbonate group possesses the requisite Lewis basicity, the position of the carbonyl oxygen in carbonate **38** is two atoms farther away from the cyclohexyl ring than it is in ester **1**. As a result, the coordination leading to ruthenacycle **136** (Scheme 10) involves a ring of six or seven members, whereas the corresponding transition state derived from carbonate **38** would require the formation of an eight- or nine-membered ring, which should be significantly less facile. Additionally, cyclooctene **51** was found to be inert to these reaction conditions, possibly due to the conformational rigidity often seen in cyclooctyl systems.³⁰

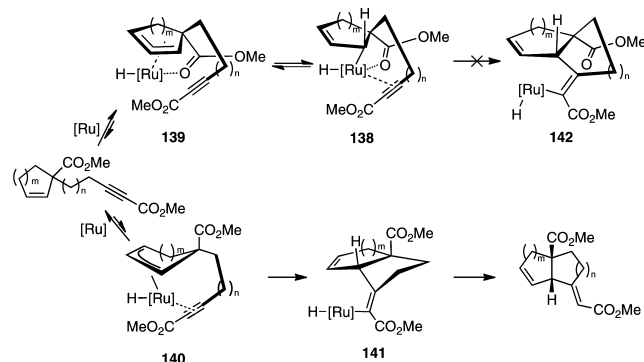
Cis Diastereoselectivity: 6,5-, 5,5-, and 5,6-Bicycles. The cis-bicyclic products formed under ruthenium catalysis can derive from one of the two mechanisms illustrated in Scheme 9: a metallacycle pathway (path A), where the intermediate **121** undergoes a β -hydride elimination of H^a prior to the final reductive elimination, or a C–H insertion pathway (path B), via **124** and **125**. The cis selectivity observed for the formation of 6,5-, 5,5-, and 5,6-bicycles could be explained by a catalytic cycle which proceeds through path A. As discussed, the body of evidence gathered up to this point suggests that, for cis-olefinic enynes, the energy barrier associated with the β -elimination of the pseudoequatorial H^b is prohibitively high. Thus, while a mechanism which proceeds via a ruthenacycle intermediate is possible and cannot be ruled out at this time, rationales within the C–H insertion manifold have been primarily considered.

It is possible that increased strain present in the 1,2-disubstituted five-membered ring (**138**, Scheme 11), as compared to the six-membered cyclohexyl intermediate **136**, causes the carboration to occur on the same side of the ring as the alkyne, yielding the observed cis-fused systems.

Scheme 11. Mechanistic Rationale for Cis Diastereoselectivity of Cyclopentenyl Enynes^a

^a E = CO₂Me; n = 0, 1; [Ru] = RuL_n. Ligands removed for clarity.

Alternatively, the 1,2-disubstituted intermediate **138** could form, but the higher level of strain³¹ involved in forming the trans-fused 5,6-, 6,5-, and 5,5-ring systems might force the reaction through a minor intermediate that ultimately leads to the observed cis-fused bicycle (Scheme 12). By rendering the carbonyl-directed insertion step (**139** → **138**) nonproductive, the reaction is forced to proceed via allylruthenium intermediate **140**, in which the carbonyl group is not bound. In this scenario, strongly coordinating groups might be expected to retard the reaction rate, as they would cause the equilibrium to lie heavily toward formation of **138**. This is consistent with the behavior of 5,6-enyne **43**, containing a strongly ligating Weinreb amide. Enyne **43** did not undergo complete conversion (see Table 10), even under extended reaction times and increased temperatures.

Scheme 12. Alternative Rationale for Cis Diastereoselectivity of 5,*n*-Systems^a

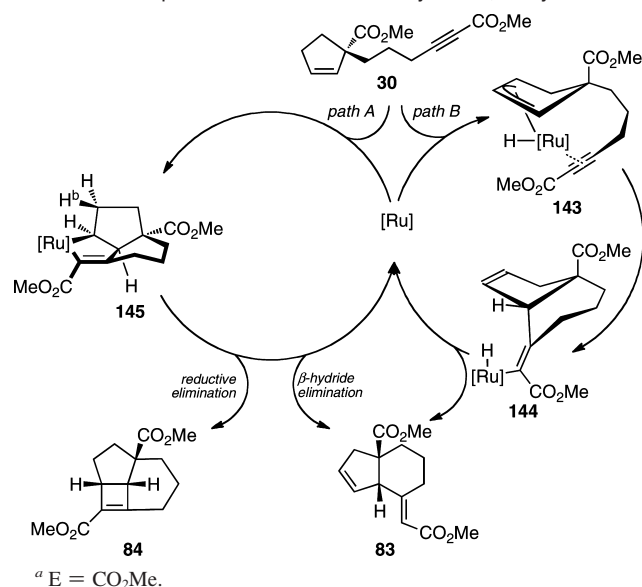
^a E = CO₂Me; m = 1, 2; n = 0, 1; [Ru] = RuL_n. Ligands removed for clarity.

Lastly, it is possible that the cis-fused 6,5-, 5,6-, and 5,5-bicyclic products are formed in the same manner as the tricyclic products are — via metallacycle formation (path A, Scheme 13). In this case, the cis-diastereomer would necessarily form. While it does not account for the requirement that the alkynes be terminated by an electron-withdrawing group, it would explain why the coordinating group is no longer required.

Product Selectivity under Ruthenium Catalysis: Bi- versus Tricycle Formation. Formation of tricycles is thought to occur via a metallacycle mechanism (path A, Scheme 13). It is likely that formation of the tricyclic product is seen only in the 5,6-system and not the 5,5-system because formation of the 5,5,4-tricycle is too high in energy. Interestingly, calculations³² of the relative energy differences between the cis-bicyclic products and the analogous tricycles revealed that the difference is smallest for the 5,6-system. The difference in energy between 5,6-bicycle **83** and tricycle **84** is calculated to be 11.2 kcal. In

(31) The higher level of strain would be present in the transition state from **138** to vinyl ruthenium **142**, not in the products. Calculations of the relative equilibrium geometry energies of the products were carried out using a Hartree–Fock basis set at the 3-21G level. These calculations showed that, for the 5,6-bicyclic system, *trans*-**83** is 3.96 kcal/mol higher in energy than *cis*-**83**; in the hydrindane system, $\Delta E_{(trans-77-cis-77)} = 11.0$ kcal/mol, and in the decalin system, $\Delta E_{(trans-2-cis-69)} = 8.68$ kcal/mol. To validate the accuracy of the 3-21G level, one set of calculations was carried out at the higher 6-31G level; the relative energies differences did not change.

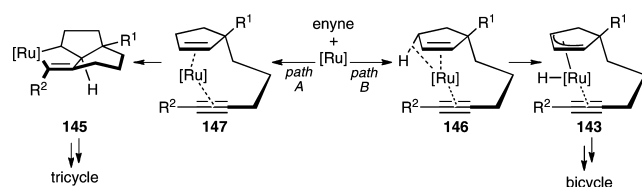
(32) Calculations of the relative equilibrium geometry energies of the products were carried out using Hartree–Fock basis sets at the 3-21G level. To validate the accuracy of the 3-21G level, one set of calculations was carried out at the higher 6-31G level; the relative energies differences did not change.

Scheme 13. Proposed Mechanistic Pathways for 5,6-Enynes^a

comparison, the tricycle that would be produced from a cycloaddition of **16** is 30.1 kcal higher in energy than the observed bicycle, *cis*-**77**. The tricycle that would derive from **1** is 18.4 kcal higher in energy than *cis*-**2**, and 9.74 kcal higher in energy than the observed *trans*-**2**.

The precise role that the DMA plays in determining the product selectivity deserves comment. It is possible that DMA, a stronger ligand than acetone, occupies the coordination site otherwise used for β -hydride elimination, thereby facilitating the C–C reductive elimination step (**145** \rightarrow **84**) of the cycloaddition (path A, Scheme 13). An alternative hypothesis is that the open coordination site required for the initial C–H insertion step of path B is occupied by a molecule of solvent. That is, the bound molecule of solvent out-competes the agostic C–H bond as a ligand.

This hypothesis, that DMA is effective because its occupation of a coordination site on the metal inhibits one of the pathways, implies that the pathways leading to tricyclic and bicyclic products have different coordination requirements. The oxidative metallacycle formation (enyne \rightarrow **145**, path A) requires that two of ruthenium's six coordination sites are unoccupied (Scheme 14). The initial coordination and insertion step (enyne \rightarrow **143**) of path B must then require more than two open sites if it is inhibited by DMA. Indeed, species **146**, in which the enyne occupies three coordination sites on the metal, is a likely intermediate. As depicted, substrate–metal interactions occur through the alkyne, the η^2 -bound olefin, and the agostic C–H bond.

Scheme 14. Coordination Requirements

This general hypothesis — that the relatively stronger ligating properties of DMA shunt the reaction through the metallacycle pathway — is in agreement with the selectivity observed for

Weinreb amide **43**, a substrate with a strong ligating group. While it failed to undergo the reaction in full conversion, enyne **43** was the only substrate that displayed any inherent product selectivity in acetone: at 71% conversion, the ratio of tricyclic to bicyclic products was 4:1 (Table 10, entry 1). The reduced reactivity of **43** would still be explained by unproductive ligation of the amide moiety to the catalyst. The role of DMA could take place while it is bound to the metal center or simply present at a nonbonding distance around the metal. If its contribution requires the ability to alternate between the two, the presence of a strong coordinating group bound so close to the reaction site could hinder the reactivity.

Finally, a unifying mechanism in which the 6,5-, 5,6-, and 5,5-bicyclic products as well as the tricyclic products are all formed from the same metallacycle intermediate (**145**, path A of Scheme 13) cannot be ruled out. If both products derive from ruthenacyclopentene **145**, the subsequent step — β -hydride elimination or reductive elimination — is product-determining. Exclusive formation of the tricyclic product by the 5,6-system is then understood in terms of the conformational differences between metallacycle **145** and the metallacycle formed from the cyclohexene-based substrates (e.g., **121b**, Scheme 9). As a result of the larger H–C–H bond angles in cyclopentane rings compared to those in cyclohexane rings, the β -hydrogen (H^b) and the metal center are placed farther apart in intermediate **145** (Scheme 13) than in metallacycle **121b**. As a consequence of the greater distance between the metal and H^b in **145**, β -hydride elimination would be kinetically disfavored, in turn allowing for reductive elimination to become a competitive process.

Conclusion

In conclusion, we have developed complementary methods for the transition-metal-catalyzed enyne cycloisomerizations of cyclic olefins. By using distinct ruthenium and palladium catalysts, decalins and 7,6-bicycles can be obtained with dichotomous stereochemical outcomes. The change in mechanism that accompanies the change in metal affords *trans*-fused 1,4-dienes with ruthenium and their *cis*-fused diastereomers under palladium catalysis. In the reactions under ruthenium catalysis, a coordinating group is required and acts to direct the metal to the same side of the carbocycle, resulting in the observed *trans* diastereoselectivity.

Subtle changes in the carbocyclic substrate led to the discovery of a heretofore-unobserved mechanistic pathway, providing bicyclic cycloisomerization products under palladium catalysis, tricyclic products under ruthenium catalysis in DMA, and a 1:1 mixture of the two under ruthenium catalysis in acetone. The different coordination requirements of the two paths allow for the reaction to be shuttled through the metallacycle pathway (generating tricyclic products) when DMA is used as a solvent. This method of obtaining these cyclobutene products complements the existing methods for catalyzing the formal [2+2] cycloaddition of alkynes. While other methods have been demonstrated for larger ring sizes with palladium, and for specific alkyne termini with platinum and gold, this method is unique in its substrate scope. To the best of our knowledge, this is the first example of a formal [2+2] cycloaddition catalyzed by CpRu(MeCN)₃PF₆.

Current efforts are directed at gaining a deeper understanding of some of the fundamental principles dictating the reactivity

of these systems, as well as extending their utility by expanding the substrate scope.

Experimental Section

General Procedure for the Ruthenium-Catalyzed Cycloisomerizations in Acetone. To a solution of the enyne substrate in acetone (0.1 M) at 23 °C under argon was added CpRu(MeCN)₃PF₆ (3–20 mol %, in general 5 mol %, all at once). The resulting mixture was stirred at room temperature for the time provided, at which point the solvent was removed via rotary evaporation. The residue was diluted in the minimum amount of CH₂Cl₂/Et₂O (1:1) and passed through a small plug of silica gel (Et₂O eluent). The filtrate was concentrated *in vacuo* to provide the cyclized adducts, which were further purified by flash chromatography.

Synthesis of Bicycle 54. According to the general procedure, 20.0 mg of **36** (0.0854 mmol) and 1.9 mg of CpRu(CH₃CN)₃PF₆ (0.00427 mmol) were stirred in 854 μL of acetone for 2 h. Purification of the residue by flash chromatography (11:1 hexanes/EtOAc eluent) afforded bicycle **54** (17.5 mg, 88% yield, *R*_f = 0.45 in 4:1 hexanes/EtOAc) as a colorless oil: ¹H NMR (400 MHz, C₆D₆) δ 9.58 (s, 1H), 5.84 (s, 1H), 5.56 (d, *J* = 10.4 Hz, 1H), 5.48–5.42 (m, 1H), 4.26 (br d, *J* = 12.7 Hz, 1H), 3.37 (s, 3H), 2.46 (br s, 1H), 1.77 (br d, *J* = 13.0 Hz, 1H), 1.73–1.54 (comp m, 3H), 1.50 (dt, *J* = 5.5, 13.1 Hz, 1H), 1.07–0.98 (m, 1H), 0.78 (dt, *J* = 5.5, 13.0 Hz, 1H); ¹³C NMR (100 MHz, C₆D₆) δ 206.0, 166.4, 160.6, 130.0, 124.9, 113.3, 51.3, 50.5, 47.9, 35.2, 33.0, 30.4, 24.7, 22.6; IR (film) 2934, 1717, 1640, 1193, 1161 cm⁻¹; HRMS (ESI⁺) *m/z* calcd for [C₁₄H₁₈O₃ + Na]⁺ 257.1154, found 257.1153.

Preparatory-Scale Example. According to the general procedure, 230 mg of **36** (0.981 mmol) and 21.3 mg of CpRu(CH₃CN)₃PF₆ (0.0491 mmol) were stirred in 9.81 mL of acetone for 2 h. Purification of the residue by flash chromatography (11:1 hexanes/EtOAc eluent) afforded bicycle **54** (189 mg, 82% yield).

General Procedure for the Ruthenium-Catalyzed Cycloisomerizations in DMA. To a solution of the enyne substrate in DMA (0.12 M) at 23 °C under argon was added CpRu(MeCN)₃PF₆ (3–20 mol %, in general 15 mol %). The resulting mixture was stirred in a preheated oil bath at 40 °C for the time provided (in general 12 h), at which point the reaction was diluted with diethyl ether and washed once with water and then once with brine. The aqueous layers were then combined and extracted once more with ether. The organic phases were combined, dried over MgSO₄, and concentrated *in vacuo*. The residue was further purified by flash chromatography to afford the cyclobutene adduct.

Synthesis of Tricycle 101. According to the general procedure, 21.0 mg of **100** (0.0741 mmol) and 4.7 mg of CpRu(MeCN)₃PF₆ (0.0107 mmol) were stirred in 618 μL of DMA for 16 h. Purification of the residue by flash chromatography (9:1 hexanes/EtOAc eluent) afforded tricycle **101** (13.8 mg, 66% yield, *R*_f = 0.45 in 17:3 hexanes/EtOAc) as a colorless oil: ¹H NMR (500 MHz, CDCl₃) δ 9.64 (s, 1H), 7.37–7.27 (comp m, 5H), 4.55–4.49 (comp m, 2H), 3.32–3.30 (br m, 1H), 3.20 (d, *J* = 9.0 Hz, 1H), 3.19 (d, *J* = 9.0 Hz, 1H), 2.84 (dm, *J* = 13.1 Hz, 1H), 2.72 (s, 1H), 2.11–2.05 (m, 1H), 2.00–1.96 (m, 1H), 1.78–1.59 (comp m, 6H), 1.45–1.40 (m, 1H); ¹³C NMR (125 MHz, CDCl₃) δ 185.2, 171.6, 138.7, 136.8, 128.4, 127.6, 127.5, 76.2, 73.4, 50.9, 45.7, 44.6, 29.0, 27.5, 27.4,

25.1, 24.3; IR (film) 2938, 2851, 1665, 1100 cm⁻¹; HRMS (ESI⁺) *m/z* calcd for [C₁₉H₂₂O₂ + Na]⁺ 305.1520, found 305.1517.

General Procedure for the Palladium-Catalyzed Cycloisomerizations. To a solution of the enyne substrate and formic acid (2 equiv) in 49:1 DCE/MeCN (0.025 M) under argon was added Pd₂dba₃·CHCl₃ (4 mol %). The resulting mixture was heated to 40 °C and stirred for the time provided. Upon completion of the reaction, the solution was cooled to room temperature and partitioned between EtOAc and saturated NaHCO₃. The aqueous phase was extracted with EtOAc, and the combined organic phases were washed with brine, dried over Na₂SO₄, and concentrated *in vacuo*. Purification of the residue by flash chromatography provided the bicyclic adduct.

Synthesis of Bicycle 70. According to the general procedure, 32.0 mg of **36** (0.137 mmol), 10.3 μL of HCO₂H (0.274 mmol), and 5.6 mg of Pd₂dba₃·CHCl₃ (0.00548 mmol) were stirred in 5.37 mL of DCE and 110 μL of CH₃CN for 5 h. Purification of the residue by flash chromatography (3:1 PhH/CHCl₃ eluent) afforded bicycle **70** (23.2 mg, 73% yield, *R*_f = 0.27 in 9:1 hexanes/EtOAc) as a colorless oil: ¹H NMR (500 MHz, CDCl₃) δ 9.44 (s, 1H), 5.83–5.78 (m, 1H), 5.73 (s, 1H), 5.57–5.53 (m, 1H), 3.68 (s, 3H), 3.16 (br s, 1H), 2.86–2.74 (comp m, 2H), 2.14–2.08 (comp m, 2H), 1.76–1.65 (comp m, 2H), 1.63–1.52 (comp m, 4H); ¹³C NMR (100 MHz, CDCl₃) δ 204.6, 167.1, 162.5, 129.0, 127.0, 116.3, 51.2, 51.1, 44.9, 28.2, 27.5, 25.3, 23.0, 22.2; IR (film) 2934, 1719, 1643, 1435, 1155 cm⁻¹; HRMS (ESI⁺) *m/z* calcd for [C₁₄H₁₈O₃ + Na]⁺ 257.1154, found 257.1148.

Synthesis of Bicycle 108. According to the general procedure, 20.0 mg of **100** (0.0706 mmol), 5.3 μL of HCO₂H (0.141 mmol), and 2.9 mg of Pd₂dba₃·CHCl₃ (0.00282 mmol) were stirred in 2.77 mL of DCE and 56.5 μL of MeCN for 2 h. Purification of the residue by flash chromatography (7:3 benzene/CHCl₃ eluent) afforded bicycle **108** (16.0 mg, 80% yield, *R*_f = 0.25 in 17:3 hexanes/EtOAc) as a colorless oil: ¹H NMR (500 MHz, CDCl₃) δ 10.0 (d, *J* = 8.9 Hz, 1H), 7.36–7.28 (comp m, 5H), 5.88 (d, *J* = 8.2 Hz, 1H), 5.82 (app dt, *J* = 2.6, 8.1 Hz, 1H), 5.49–5.46 (m, 1H), 4.52 (s, 2H), 3.40 (d, *J* = 9.0 Hz, 1H), 3.35 (d, *J* = 9.0 Hz, 1H), 3.26 (s, 1H), 3.11–3.05 (m, 1H), 2.49 (app dq, *J* = 2.6, 16.5 Hz, 1H), 2.35–2.28 (m, 1H), 2.13 (app dq, *J* = 2.2, 16.5 Hz, 1H), 1.77–1.65 (comp m, 2H), 1.60–1.49 (comp m, 2H); ¹³C NMR (125 MHz, CDCl₃) δ 168.0, 132.2, 128.4, 127.6, 127.5, 127.3, 75.4, 73.3, 57.4, 49.9, 43.7, 30.8, 26.0, 22.2; IR (film) 2929, 2851, 1671, 1101 cm⁻¹; HRMS (ESI⁺) *m/z* calcd for [C₁₉H₂₂O₂ + Na]⁺ 305.1512, found 305.1514.

Acknowledgment. We thank the American Cancer Society for a postdoctoral fellowship for E.M.F. We also thank the NSF and NIH (GM13598) for the support of our programs, and Johnson Matthey for the generous donation of metal salts.

Supporting Information Available: Experimental procedures, compound characterization data, and spectra. This material is available free of charge via the Internet at <http://pubs.acs.org>.

JA103663H